(6, 12), and hence tend to act as one component. Similarly, the two minerals in each pair contain components that are either indistinguishable [CCFXe in chromite and carbon (6)] or very similar [trapped xenon in polymer and Q (7)], and so even samples of quite diverse mineralogy still tend to lie on the mixing line.
12. R. S. Lewis, L. Alaerts, E. Anders, in *Lunar Science IX* (Lunar Science Institute, Houston, 1978), p. 645.
13. D. D. Clayton and R. A. Ward, *Astrophys. J.*, in press.
14. A. G. W. Cameron, *Space Sci. Rev.* **15**, 121 (1973).
15. Krypton-86 is a mixture of trapped and fission components only, of the isotopic composition given in (7). The amount of the fission Kr component is calculated from the fission Xe component found previously, using an $(^{86}Kr/^{136}Kr)_f$ of 0.31 ± 0.09 (7).
16. D. C. Black and R. O. Pepin, *Earth Planet. Sci. Lett.* **6**, 395 (1969); D. C. Black, *Geochim. Cosmochim. Acta* **36**, 377 (1972); P. Eberhardt, *Earth Planet. Sci. Lett.* **24**, 182 (1974); F. Niederer and P. Eberhardt, *Meteoritics* **12**, 327 (1977). The latter authors observed a $^{21}Ne/^{22}Ne$ ratio of 0.0211 in a carbonaceous fraction from the Dimmitt H3 chondrite.
17. V. Trimble, *Rev. Mod. Phys.* **47**, 877 (1975).
18. U. Frick, R. K. Moniot, J. M. Neil, D. L. Phinney, J. H. Reynolds, *Geochim. Cosmochim. Acta*, in press; P. M. Jeffery and E. Anders, *ibid.* **34**, 1175 (1970).
19. R. Göbel, U. Ott, F. Begemann, *J. Geophys. Res.* **83**, 855 (1978).
20. I. Iben, Jr., *Astrophys. J.* **147**, 624 (1967); ——— and J. W. Truran, *ibid.* **220**, 980 (1978).
21. B. Srinivasan, R. S. Lewis, E. Anders, *Geochim. Cosmochim. Acta* **42**, 183 (1978).
22. L. H. Fuchs, E. Olsen, K. J. Jensen, *Smithson. Contrib. Earth Sci. 10* (1973), p. 13.
23. R. Clegg and S. Wyckoff, *Mon. Not. R. Astron. Soc.* **179**, 417 (1977).
24. L. Grossman and J. W. Larimer, *Rev. Geophys. Space Phys.* **12**, 71 (1974).
25. J. W. Larimer and M. Bartholomay, *Geochim. Cosmochim. Acta*, in press.
26. J. M. Lattimer, D. N. Schramm, L. Grossman, *Astrophys. J.* **219**, 230 (1978).
27. R. N. Clayton, L. Grossman, T. K. Mayeda, *Science* **182**, 485 (1973); R. N. Clayton, N. Onuma, L. Grossman, T. K. Mayeda, *Earth Planet Sci. Lett.* **34**, 209 (1977); R. N. Clayton and T. K. Mayeda, *Geophys. Res. Lett.* **4**, 295 (1977).
28. G. J. Wasserburg, T. Lee, D. A. Papanastassiou, *Geophys. Res. Lett.* **4**, 299 (1977); T. Lee, D. A. Papanastassiou, G. J. Wasserburg, *Astrophys. J.* **211**, L107 (1977).
29. R. N. Clayton, T. K. Mayeda, S. Epstein, in *Lunar Science IX* (Lunar Science Institute, Houston, 1978), p. 186.
30. T. Lee, D. A. Papanastassiou, G. J. Wasserburg, *Astrophys. J.* **220**, L21 (1978).
31. C. E. Rees and H. G. Thode, *Geochim. Cosmochim. Acta* **41**, 1679 (1977).
32. M. T. McCulloch and G. J. Wasserburg, *Astrophys. J.* **220**, L15 (1978).
33. G. W. Lugmair, K. Marti, N. B. Scheinin, in *Lunar Science IX* (Lunar Science Institute, Houston, 1978), p. 672; D. A. Papanastassiou, J. C. Huneke, T. M. Esat, G. J. Wasserburg, in *ibid.*, p. 859.
34. D. D. Clayton, *Astrophys. J.* **199**, 765 (1975); *Icarus* **32**, 255 (1977).
35. H. Takahashi, H. Higuchi, J. Gros, J. W. Morgan, E. Anders, *Proc. Natl. Acad. Sci. U.S.A.* **73**, 4253 (1976).
36. C. H. Townes, *Observatory* **97**, 52 (1977).
37. R. A. Canalas, E. C. Alexander, Jr., O. K. Manuel, *J. Geophys. Res.* **73**, 3331 (1968); D. Phinney, *Earth Planet. Sci. Lett.* **16**, 413 (1972).
38. R. A. Ward, M. J. Newman, D. D. Clayton, *Astrophys. J. Suppl. Ser.* **31**, 33 (1976); D. D. Clayton, W. A. Fowler, T. E. Hull, B. A. Zimmerman, *Ann. Phys. (N.Y.)* **12**, 331 (1961).
39. P. Lee, *Astrophys. J.* **192**, 133 (1974).
40. R. N. Clayton, *Science* **140**, 192 (1963); A. G. W. Cameron, in *Interstellar Dust and Related Topics*, J. M. Greenberg and H. C. Van de Hulst, Eds. (Reidel, Dordrecht, 1973), p. 545; ——— and J. W. Truran, *Icarus* **30**, 447 (1977).
41. A 4.72-mg sample of Murchison residue 1C10 was heated for 30 minutes at each of the temperatures indicated, to extract noble gases. Concentrations are accurate to ± 20 percent for He and ± 10 percent for all other gases.
42. P. A. Seeger, W. A. Fowler, D. D. Clayton, *Astrophys. J. Suppl. Ser.* **11**, 121 (1965).
43. B. J. Allen, J. H. Gibbons, R. L. Macklin, *Adv. Nucl. Phys.* **4**, 205 (1971).
44. J. A. Holmes, S. E. Woosley, W. A. Fowler, B. A. Zimmerman, *At. Data Nucl. Data Tables* **18**, 305 (1976).
45. V. Benzi, R. d'Orazzi, G. Reffo, M. Vaccari, unpublished work cited in (13).
46. We are indebted to J. Gros for preparation of the sample, to R. S. Lewis for the x-ray diffraction pattern, and to D. N. Schramm for advising us of some potential paradoxes raised by our data. One of us (B.S.) thanks the University of Missouri for releasing time to allow completion of this report. This work was supported in part by NASA grant NGL-14-001-010.
* Present address: Department of Chemistry, University of Missouri, Rolla 65401.

8 February 1978

## Seismic Amplitude Measurements Suggest Foreshocks Have Different Focal Mechanisms than Aftershocks

Abstract. *The ratio of the amplitudes of* P *and* S *waves from the foreshocks and aftershocks to three recent California earthquakes show a characteristic change at the time of the main events. As this ratio is extremely sensitive to small changes in the orientation of the fault plane, a small systematic change in stress or fault configuration in the source region may be inferred. These results suggest an approach to the recognition of foreshocks based on simple measurements of the amplitudes of seismic waves.*

Significant progress has been made in the recognition of long-term recurrence patterns of large earthquakes (*1*), and promising results are slowly accumulating which suggest that intermediate-term changes (years to months) in regional seismicity, strain, and electromagnetic measurements may provide intermediate-term precursors (*2, 3*). However, the fact remains that short-term precursors (days to hours) will be needed to allow evacuation of unsafe structures, if significant reductions are to be made in loss of life and human suffering. The recent Chinese success in predicting the Haicheng earthquake (4 February 1975, magnitude $M = 7.3$) was based on the use of long-, intermediate-, and short-term precursors. The imminent prediction was based partly on the recognition of a swarm of small to moderate earthquakes near Haicheng as a potential foreshock sequence (*4*). However, foreshocks do not always occur; estimates on their frequency vary widely (*3, 5, 6*), and they are usually recognizable as foreshocks only in hindsight. To use foreshocks in a predictive mode, one must distinguish them from background seismicity and earthquake swarms (*7*).

In earlier work along the line reported here, Nersesov and his colleagues found large changes in the orientation of focal mechanisms over a large region prior to thrust earthquakes in Central Asia (*8*). Similar changes have recently been reported prior to an earthquake of magnitude 5 in the Central Aleutians (*9*). A retrospective study of the Haicheng foreshocks indicates that they were distinguishable from similar earthquake swarms on the basis of remarkably consistent focal plane solutions (*4, 10*). Other possible changes in compressional or shear wave amplitudes, or both, before large earthquakes have been reported from Kamchatka and China (*11*).

We summarize here work on small foreshocks to three moderate California earthquakes (Fig. 1, a to d) which shows that the mean nodal plane orientations were different from those of comparable aftershocks (*12*). In each case the inferred changes were small (5° to 10°) and were inferred from changes in the ratio of compressional to vertically polarized shear-wave amplitudes (*P/SV*), as recorded from nearby short-period vertical seismometers. Unfortunately, it was not possible to find small earthquakes prior to the foreshocks at the same location with which to establish "normal" background values. Therefore, it is not possible to assess whether our observations would have been of use in identifying the foreshocks as such in advance, but only that they can be used to distinguish foreshocks from aftershocks. Our observations do demonstrate, however, a simple procedure for monitoring small changes in the fault plane orientations of local earthquakes. This procedure may provide an approach to the observation of stress changes at depth preceding, accompanying, and following large earthquakes, a problem that lies directly at the core of the earthquake prediction question.

The Oroville earthquake (local magnitude $M_L = 5.7$) occurred at 2020 Greenwich mean time (G.M.T.) on 1 August 1975, in the western foothills of the Sierra Nevada, 15 km south of the town of Oroville, California. The aftershocks occurred within a planar band striking north-south and dipping steeply to the west; fault plane solutions indicate predominantly normal dip-slip motion on this plane (*13*). The main shock was preceded by 58 recorded foreshocks over a period of 4 weeks, starting on 28 June. They ranged from $M_L = 0.5$ to $M_L = 4.7$


0036-8075/78/0707-0056$00.50/0 

and were located inside a cube 4 km on a side centered at 39°27′N, 121°31′W at a depth of 8 km (Fig. 1b).

The mean *P/SV* ratio at station KPK for 27 foreshocks was 1.08 (± 61 percent); this ratio decreased to 0.39 (± 46 percent) for 55 aftershocks from the same cube (Fig. 2a) (*14*). This change and a smaller change at station ORV are consistent with a clockwise rotation of 10° to 20° in the strike of the fault plane and a simultaneous change in the orientation of the slip vector (in the sense of adding a left-lateral component to the aftershock mechanisms) at the time of the main event (Fig. 1b).

The Galway Lake earthquake ($M_L$ = 5.2) occurred at 0138 G.M.T. on 1 June 1975 in the central Mojave Desert. The aftershocks occurred in an elliptical zone striking north-northwest. Fault plane solutions indicate predominantly right-lateral strike-slip faulting on planes dipping steeply to the west-southwest. The main event was preceded by nine located foreshocks, ranging in magnitude from $M_L$ = 1.9 to $M_L$ = 3.4, occurring over a period of 12 weeks starting on 9 March 1975. All of the foreshocks and the aftershocks whose amplitudes are reported here cluster inside a cube measuring 1 by 1 by 2 km$^3$, centered at 34°31.3′N, 116°29.5′W at a depth of 2 km; this cube also encloses the hypocenter of the main shock (Fig. 1c).

The mean *P/SV* ratio at station TPC for nine foreshocks was 1.16 (± 9 percent); this value decreased to 0.72 (± 40 percent) for 28 aftershocks (Fig. 2b). This change and all the other amplitude and first motion data that we studied are consistent with a counterclockwise rotation of 5° to 10° in the strike of the fault plane at the time of the main event (Fig. 1c). [Sixteen aftershocks between 6 and 30 June, when the amplitudes show less scatter, had a mean of 0.38 (± 16 percent); this value corresponds to a somewhat larger rotation in the same direction.] A change in dip of the fault plane can also be used to fit the observations, although not as well.

The Briones Hills earthquake ($M_L$ = 4.3) occurred at 0938 G.M.T. on 8 January 1977 near Berkeley, California. The aftershocks lie in a narrow zone extending 2 km in the direction 5° west of north. They range in depth from 7 to 10 km and dip steeply to the west; the fault plane solution for the main event indicates predominantly right-lateral strike-slip motion on this plane with a small component of normal faulting (Fig. 1d) (*15*). During the 8 hours prior to the main event, ten foreshocks of magnitude greater than $M_L$ = 0.5 were recorded. The largest had a magnitude of $M_L$ = 4.0 and occurred 40 minutes prior to the main event.

The *P/SV* ratio at station BKS for six foreshocks was 0.53 (± 23 percent); 30 aftershocks had a mean value of 0.29 (± 34 percent) (Fig. 2c). This change, plus first motion reversals at a number of stations, are sufficient to require a counterclockwise rotation of the fault plane of 5° to 10° at the time of the main event (Fig. 1d). Amplitude and first motion changes at the next nearest station (station BWR) are consistent with a small change in slip vector orientation at the same time.

In the above discussion we have attributed the observed amplitude changes to rotations of the focal mechanisms of the source earthquakes. Alternatively, attenuation changes in the material surrounding the source might have occurred; such phenomena have recently been observed in laboratory samples approaching failure (*16*). In two of the cases discussed here (Oroville and Briones) the amplitude changes were accompanied by simultaneous first motion changes at one or more nearby stations. In addition, in all three cases, changes were also noted in the ratio of *P* wave amplitudes recorded at two different stations. Although these data are in support of the source orientation explanation, they are not sufficient to totally exclude an attenuation change, particularly in light of work elsewhere which would seem to favor such an explanation (*11*, *16*). A definitive discrimination between these two classes of models will probably only be possible when recordings of foreshock first motions and amplitudes are available from many stations.

Another source of apparent amplitude

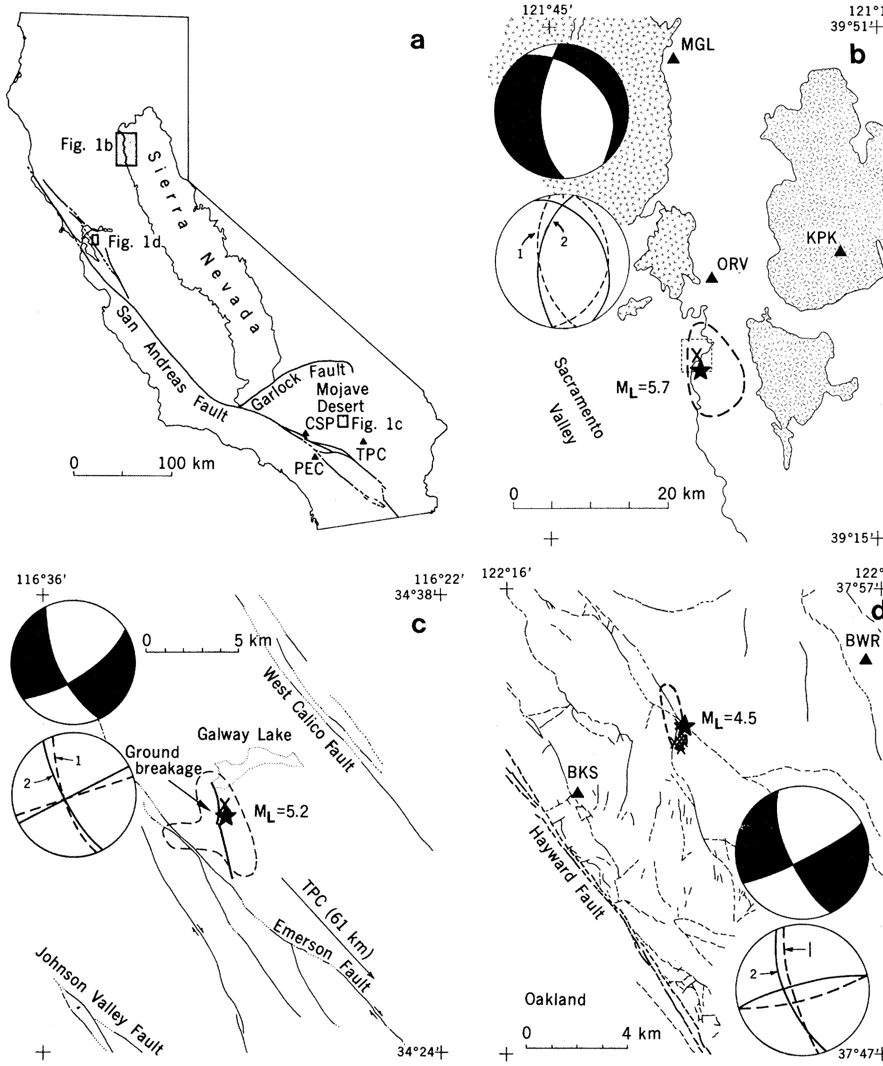


Fig. 1. (a) Map of California showing the major faults and the locations of three areas studied. (b) Map of the Oroville area, showing the seismic stations used, location of the foreshocks (X), the main event (star), the aftershock zone (heavy dashed line), and the fault plane solution of the main event. Also shown are the average nodal plane orientations for the foreshocks (*1*, dashed line) and aftershocks (*2*, solid line). (c) Map of the central Mojave Desert, showing the location of the Galway Lake earthquake. Other features are as in (b). (d) Map of the San Francisco Bay area, showing the location of the Briones Hills earthquake. Other features are as in (b).

changes which would have nothing to do with either source orientations or material property changes would arise if a systematic difference existed between the depths (or other hypocentral parameters) of the foreshocks and the aftershocks to which they are compared. We have examined this possibility at some length at Oroville and Briones, where the foreshock depths are reasonably well constrained, and it does not contribute to the observed amplitude changes. At Galway Lake the question is more difficult, in view of the very shallow depths of the earthquakes and the distance to the nearest station that recorded the foreshocks.

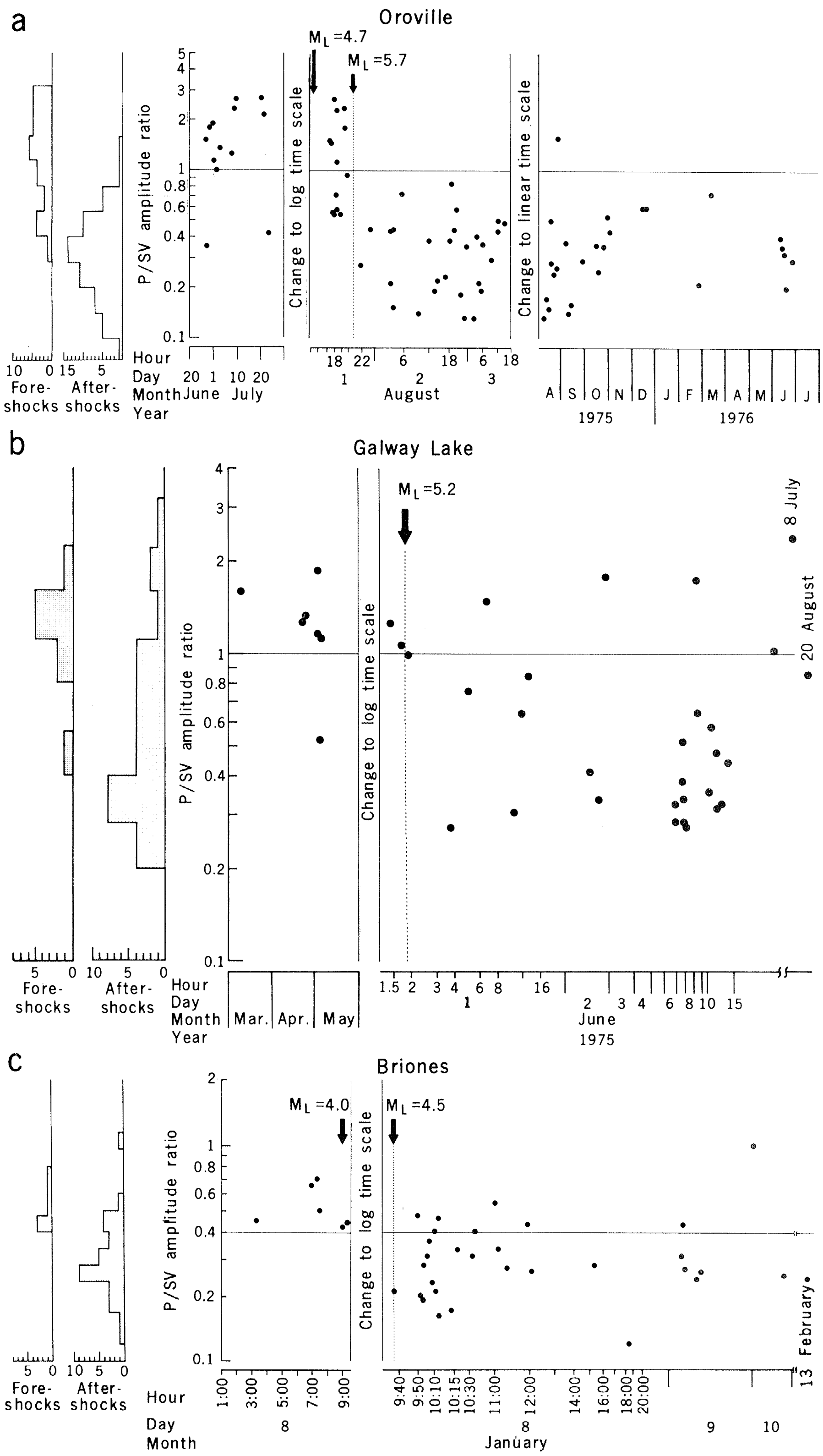


Fig. 2. Plots of the amplitude ratio, *P/SV*, for various periods of time spanning the three earthquakes discussed. To the left are histograms of foreshock and aftershock amplitudes. (Note the changes between linear and logarithmic time scales.) (a) Amplitudes at station KPK spanning the Oroville earthquake. (b) Amplitudes at station TPC spanning the Galway Lake earthquake. (c) Amplitudes at station BKS spanning the Briones Hills earthquake.

In addition to the inferred fault plane rotations, several other aspects of these three foreshock sequences are of interest. For 4 days prior to the Haicheng earthquake, foreshocks were recorded which had very consistent *P/SV* ratios at a large number of local and regional seismic stations. Aftershocks from the same approximate location exhibited a great deal of scatter (*4, 10*). Two of the earthquakes studied here (Galway Lake and Briones) exhibited possibly similar behavior (Fig. 2, b and c), whereas the Oroville earthquake did not (Fig. 2a). Thus, our data are ambiguous on this point and more data will be required to assess its general applicability.

Another feature of the foreshock sequences discussed here is that in each case all of the foreshocks were located within a very small hypocentral volume, which either included or was immediately adjacent to the hypocenter of the main event. This type of foreshock behavior has often been noted, and these foreshocks may form a distinct subset of foreshocks, taken in the broader sense of small earthquakes that precede large ones (*5, 17*). In addition, although the scatter in the amplitude ratios shown in Fig. 2 appears large, when mapped into changes in source orientation it corresponds to variations of only a few degrees. This remarkable and unexpected stability suggests that amplitudes recorded from local earthquakes may contain invaluable information concerning small changes in stress orientation at depths where it will probably never be possible to measure them directly. In addition, they may be of practical use in the identification of a foreshock sequence, if it can be established that foreshock amplitude ratios differ in some respect from "normal" background values, and not just when compared to aftershocks as they were here.


ALLAN LINDH

*U.S. Geological Survey, Menlo Park, California 94025, and Geophysics Department, Stanford University, Stanford, California 94305*

GARY FUIS

*U.S. Geological Survey, Seismological Laboratory, California Institute of Technology, Pasadena 91125*

CONSTANCE MANTIS

*U.S. Geological Survey, Menlo Park, California 94025*

### References and Notes

1. S. A. Fedotov, *Tr. Inst. Fiz. Zemli Akad. Nauk SSSR* **66** (No. 36) (1965); C. Allen, P. Saint-Amand, C. Richter, J. Nordquist, *Bull. Seismol. Soc. Am.* **55**, 753 (1956); K. Mogi, *Bull. Earthquake Res. Inst. Tokyo Univ.* **47**, 395 (1969); J. Kelleher, L. Sykes, J. Oliver, *J. Geophys. Res.* **78**, 2547 (1973).
2. For example, C. E. Mortensen and M. J. S. Johnston, *J. Geophys. Res.* **81**, 3561 (1976); B. E. Smith and M. J. S. Johnston, *ibid.*, p. 3556; W. Thatcher, *ibid.* **80**, 4862 (1975).
3. T. Rikitake, *Earthquake Prediction* (Elsevier, Amsterdam, 1976).
4. Haicheng Earthquake Study Delegation, *EOS (Trans. Am. Geophys. Union)* **58**, 236 (1977).
5. C. F. Richter, *Elementary Seismology* (Freeman, San Francisco, 1958).
6. K. Mogi, *Bull. Earthquake Res. Inst. Tokyo Univ.* **41**, 615 (1963); L. Jones and P. Molnar, *Nature (London)* **262**, 677 (1976).
7. In this report the term "foreshocks" is used in the limited sense of earthquakes that occur at essentially the same hypocenter as the main event and whose relation in time to both the main event and background seismicity is such that they can be unequivocally associated with the main event. Although this definition would not cover all circumstances, it is sufficient here. More detailed accounts of this work are presented elsewhere: A. G. Lindh and C. E. Mantis, in preparation; G. S. Fuis and A. G. Lindh, in preparation.
8. M. A. Sadovsky *et al.*, *Tectonophysics* **14**, 295 (1972).
9. E. R. Engdahl and C. Kisslinger, *J. Phys. Earth*, in press.
10. Jin Yan, Zhao Yi, Chen Yong, Yan Jai-Quan, Zhou Yu-ru, *Acta Geophys. Sin.* **19**, 156 (1976).
11. S. A. Fedotov, A. A. Gusev, S. A. Boldyrev, *Tectonophysics* **14**, 279 (1972); S. A. Fedotov *et al.*, *ibid.* **37**, 305 (1977); Feng Te-yi, *Acta Geophys. Sin.* **17**, 140 (1974) (this article includes an extensive discussion of the relation between focal plane solutions and *P* and *S* waves from local earthquakes, although the premonitory changes reported are attributed to attenuation changes).
12. Amplitudes of seismic waves recorded at a given station vary as a function of both the earthquake source orientation and location. Since we were looking for small changes in orientation, it was necessary to minimize the effects of location. For this reason, we compared foreshock amplitude ratios to amplitude ratios from aftershocks at the same approximate location. In practice, events were used from a cube a few kilometers on a side.
13. C. G. Bufe, F. W. Lester, K. M. Lahr, J. C. Lahr, L. C. Seekins, T. C. Hanks, *Science* **192**, 72 (1976); K. Lahr *et al.*, *Bull. Seismol. Soc. Am.* **66**, 1085 (1976); C. Langston and R. Butler, *ibid.*, p. 1111.
14. The averages shown are estimates of the logarithmic mean, $(\overline{P/S})_{\log}$; the uncertainties shown are estimates of the fractional standard deviation $\sigma_{\log}/(\overline{P/S})_{\log}$. They were obtained as follows: $R = \ln (P/S)$, $\delta R^2 = \delta P^2/P^2 + \delta S^2/S^2$, where $P$ and $S$ are the amplitudes measured for a given event, and $\delta P$ and $\delta S$ are estimates of their respective uncertainties. $\bar{R} = \Sigma wR/\Sigma w$, where $w_i = (\delta R_i)^{-2}$, and $\sigma_R{}^2 = (\Sigma wR^2 - \bar{R}\Sigma wR)/\Sigma w$; then $(\overline{P/S})_{\log} = \exp (\bar{R})$ and $\sigma_{\log} = \bar{R}\sigma_R$. The uncertainties shown are thus estimates of the standard deviation of the data. If one wished to estimate the significance of the changes in the mean, he could obtain the standard deviation of the mean by dividing by the square root of the number of observations. We have not attempted such a calculation here, primarily because the data do not have a true log-normal distribution. Fortunately, in at least some of the cases shown, the change is large enough to not require statistics.
15. B. Bolt, J. Stifler, R. Uhrhamer, *Bull. Seismol. Soc. Am.* **67**, 1555 (1977); A. Lindh and C. Mantis, in preparation.
16. D. A. Lockner, J. B. Walsh, J. D. Byerlee, *J. Geophys. Res.* **82**, 5374 (1977).
17. T. V. McEvilly, W. M. Bakun, K. B. Casaday, *Bull. Seismol. Soc. Am.* **57**, 1221 (1967); C. G. Allen and J. M. Nordquist, *U.S. Geol. Surv. Prof. Pap.* 787 (1972), pp. 16–23.
18. We thank B. Raleigh and W. Thatcher for help and encouragement with this work; D. Boore, T. Hanks, and B. Bakun for critical reading of the manuscript; B. Bolt for a preprint of his paper and permission to use data from the Berkeley Seismograph Station; P. Morrison for his help and cooperation with data from stations operated by the California State Department of Water Resources; and R. Eis and D. Barton for expert technical assistance. Conversations with I. L. Nersesov, D. Lockner, and J. Byerlee provided much of the incentive for this work.


28 December 1977; revised 14 March 1978

## Daylight Time-Resolved Photographs of Lightning

Abstract. *Lightning dart leaders and return strokes have been recorded in daylight with both good spatial resolution and good time resolution as part of the Thunderstorm Research International Program. The resulting time-resolved photographs are apparently equivalent to the best data obtained earlier only at night. Average two-dimensional return stroke velocities in four subsequent strokes between the ground and a height of 1400 meters were approximately $1.3 \times 10^8$ meters per second. The estimated systematic error is 10 to 15 percent.*

Time-resolved photographs of lightning leaders and return strokes in the daytime are practically nonexistent. However, photographs of the entire lightning flash in the daytime are well documented (*1, 2*). They have been used primarily to obtain channel characteristics, such as shape, number of branches, and ground contact point, and have necessarily integrated all the light from the flash. Successful experiments to time-resolve the leaders and return strokes in a flash have been restricted to nighttime observations (*3, 4*). These data have typically yielded leader and return stroke velocities, which are among the fundamental physical characteristics of lightning.

Recent interest in the return stroke velocity has been stimulated by the realization that another physical characteristic of lightning, the electric current, can be remotely determined in the first few tens of microseconds in a straight, vertical cloud-to-ground return stroke if the electric radiation field and return stroke velocity are known (*5*). The electric radiation field is now routinely measured at the National Aeronautics and Space Administration (NASA) Kennedy Space Center as part of the summer Thunderstorm Research International Program (TRIP). Velocity measurements correlated with these measurements of the electric radiation field will help to verify that the computational techniques used to obtain the current are valid. The thunderstorm activity typically peaks in the early afternoon in July and August (*6*). Unfortunately, because thunderstorms tend not to occur during the nighttime, reliable return stroke velocities have not yet been reported in these experiments. Consequently, the remote determination of electric current in return strokes in the TRIP experiments depends upon recording in the daytime the luminous components in a flash and subsequently measuring their velocities. We present here the first daytime recordings of dart leaders and return strokes with both good spatial resolution and good time resolution.

Our equipment consists of a streaking camera (Beckman and Whitley model 351) and a data-back still camera (Nikon), both loaded with Kodak 2476 Shellburst film. Excess fogging during the exposure is prevented by the use of a conventional No. 92 gelatin filter, a deep red filter which passes only light of wavelength greater than approximately 620 nm (*1*). Each camera is equipped with a 55-mm objective lens, and the shutters are triggered by an electronic circuit which is activated by light from the first return stroke. The light is detected by a solar cell consisting of 2 cm$^2$ of silicon on a ceramic base and mounted with a field of view of approximately 35°. The resulting amplified current signal is used to trigger the streaking camera, the still camera, and a digital timer for sight-sound measurements of the distance to the flash. The amplified signal for the streaking camera is used to trigger a silicon-controlled rectifier which discharges a capacitor across a solenoid, opening the leaf shutter in 10 msec. The exposure is typically set for 0.1 second and *f*/2 to record, on the average, at least two subsequent strokes in a multistroke flash composed of three or more strokes. The drum in the streaking camera is rotated at 50 rev/sec to produce a writing rate of $4.3 \times 10^{-2}$ mm/$\mu$sec. The amplified signal for the still camera is used to close a contact and open the focal plane shutter in approximately 55 msec. We can vary the exposure by monitoring a through-the-lens meter, but typically the exposure is 0.5 second at *f*/32. This system will not record the first stroke but is adequate for recording and time-resolving subsequent strokes in most multistroke flashes. The resulting photographs and distance measurements can be used to calculate the velocity of the luminous events in a flash.

Figure 1 shows a flash recorded in the afternoon at approximately 1831 U.T. on 22 July 1977 from the top of the Opera-